Soft Matter

Accepted Manuscript

This article can be cited before page numbers have been issued, to do this please use: B. Jeong, Y. Zhao and S. Dai, *Soft Matter*, 2026, DOI: 10.1039/D6SM00408C.

ROYAL SOCIETY OF CHEMISTRY

rsc.li/soft-matter-journal

View Article Online
DOI: 10.1039/D6SM00408C

Prepared for *Soft Matter*

Words: 4896

Figures: 7

Tables: 1

TITLE:

Rheology of *Escherichia coli* suspensions with various bacterial morphologies and motion characteristics

AUTHOR NAMES AND AFFILIATIONS:

Boyoung Jeong[a,c], Yumeng Zhao[b,c], and Sheng C. Dai[c*]

[a] Department of Civil, Architectural, and Environmental Engineering, Illinois Institute of Technology, Chicago, IL 60616, United States

[b] Department of Civil and Environmental Engineering, University of Nebraska-Lincoln, Lincoln, NE 68588, United Sates

[c] School of Civil and Environmental Engineering, Georgia Institute of Technology, Atlanta, GA 30332, United States

View Article Online
DOI: 10.1039/D6SM00408C

ABSTRACT:

Motile bacteria can interact with surrounding fluids, creating complex rheological behavior of suspensions. Yet such studies with paralyzed flagella or de-flagellated bacteria are limited, leaving the separate roles of motility, flagella, and cell morphology poorly resolved. This study experimentally investigates the rheology of bacterial suspensions using three strains of *Escherichia coli* (*E. coli*), ATCC9637 motile with rotating flagella, HCB136 non-motile mutant with paralyzed flagella, and HCB137 non-motile mutant without flagella, to understand the role of bacterial morphology and motility in suspension rheological behaviors. The results show that the ATCC9637 suspension exhibits a notable decrease in viscosity, particularly pronounced in the low shear rate regime, whereas the HCB136 suspension shows an increase in viscosity, especially in concentrated suspensions. This contrast underscores the influence of active swimmers in modifying the flow field and subsequently fluid viscosity. Deflagellated bacteria reduce fluid viscosity, despite the absence of the organelles necessary for propulsion, driven by flow-induced collective behavior arising from their elongated body shape. Two dimensionless numbers Pe_{f1} and Pe_{f2} are introduced to delineate the bacterial stress dominant and flow stress dominant regimes along the normalized shear rate. Finally, a prediction model is formulated to correlate the viscosity of bacterial suspensions with shear rate, cell concentration, bacterial morphology, and bacterial motility.

KEYWORDS:

Rheology; *Escherichia coli*; Bacterial suspension; Motility.

View Article Online
DOI: 10.1039/D6SM00408C

1. INTRODUCTION

Bacteria suspended in fluids constantly interact with their surrounding environment [1, 2]. Hydrodynamic interactions between bacterial cells and the suspension fluids, as well as bacterial behaviors such as cell attraction, collision, and collective motion, modify the local flow field. This gives rise to non-linear, complex rheological behavior observed in bacterial suspensions [3-6]. Because of their unique flow behavior, bacterial suspensions have attracted increasing interest in studying across physics, biology, and ecology, with potential applications in medical and energy-related fields [6][7][8][9][10, 11].

The non-Newtonian nature of active particle suspensions was described two decades ago using a theoretical equation for the rheological behaviors of active suspensions arising from the forces associated with the active particles [12]. Subsequent theoretical investigations indicated that the asymmetric shape and self-propulsion of active particles contribute to the shear-thinning or shear-thickening behavior in active suspensions. Pusher swimmers produce a net negative stresslet that reduces the shear stress needed to drive flow, and consequently decreases the viscosity. On the other hand, puller swimmers generate the positive stresslet and increase fluid viscosity [13-16]. These predictions suggested that suspensions with pusher bacteria like *Escherichia coli* (*E. coli*) and *Bacillus subtilis* exhibit decreased viscosity [17, 18], whereas suspensions with puller swimmers such as *Chlamydomonas reinhardtii* also display increased viscosity [19]. Additional experimental and theoretical investigations have been conducted, considering various factors such as motor characteristics [20], background fluid conditions [21], and external cell behaviors, including collective motion [22], hydrodynamic collision [23], and diffusive motion [24].

Studies on the rheology of bacterial suspensions have primarily focused on swimming bacteria with rotating flagella, demonstrating that bacterial activity can alter suspension viscosity. However, the specific contributions of bacterial motility, flagella, and cell morphology remain insufficiently understood, partly because relatively few studies have examined nonmotile bacteria. For example, the suspension viscosity of nonmotile bacteria, specifically an asphyxiated *E. coli* strain treated with sodium azide (NaN_3), demonstrated no viscosity reduction [25]. Several studies utilized nonmotile mutant *E. coli* strains to examine the effects of flagella and motility, and these investigations centered on cell attachment and

View Article Online
DOI: 10.1039/D6SM00408C

detachment [26], retardation and dispersion [27], and diffusion [28], rather than suspension rheology.

In addition, many experimental observations have been performed in solutions supplemented with the polyvinylpyrrolidone polymer [17, 21, 26], which has a higher viscosity than water and exhibits less variation in viscosity with shear rate. However, they are less representative of water-like environments relevant to many natural and engineered applications. Accurate viscosity measurements in water-based solutions are also challenging because water presents high viscosity at very low shear rate due to the surface tension, which can generate a torque that is more than two orders of magnitude greater than the torque arising from material deformation, particularly influencing viscosity measurements in rotational rheometers [29]. Therefore, a clearer understanding and accurate measurements of the bacterial suspension rheology in water-like solutions, without added polymers, is needed to improve the interpretation and broader applicability of active particle suspensions studies.

Despite extensive work on motile bacterial suspensions, the individual roles of self-propulsion, the flagellar apparatus itself, and cell-body geometry have rarely been separated. As a result, it remains unclear whether the rheological signatures attributed to active swimming stresses, from the passive hydrodynamic presence of flagella, or simply from the elongated, anisotropic shape of the cells. Resolving this ambiguity requires a controlled comparison among bacteria that share a common morphology but differ in well-defined motility and flagellar traits, measured in a water-like medium free of viscosity-enhancing polymers. To address this, we examine the rheology of bacterial suspensions using three *E. coli* strains with distinct shape and motion characteristics: motile *E. coli* with rotating flagella (ATCC9367), non-motile *E. coli* mutant with paralyzed flagella (HCB136), and non-motile *E. coli* mutant without flagella (HCB137). By comparing these strains in water-based solution, this study decouples motility, flagellar presence, and cell geometry on suspension viscosity under environmentally relevant fluid conditions. The resulting data are used to establish a prediction model that enables a unified, motility- and morphology-aware description of suspension rheology spanning both active and passive regimes.

View Article Online
DOI: 10.1039/D6SM00408C

2. MATERIALS AND METHODS

2.1 Bacterial growth and sample preparation

This study selected three *E. coli* strains with varying morphology and motility characteristics: *E. coli* ATCC9637, a motile strain, and two mutants, *E. coli* HCB136 and *E. coli* HCB137, as non-motile strains. *E. coli* HCB136 possesses a complete flagellar structure but is paralyzed due to a mutation in the *motB580* gene, while *E. coli* HCB137 lacks the flagella entirely due to the deletion of Δ*flhC-flhA* and the MotA-MotB complex [28].

To prepare bacterial suspensions, *E. coli* strains were cultured in the appropriate medium at 37°C (the optimum temperature for growth), 180 rpm, and 1 atm for 16-18 h. *E. coli* ATCC9637 was grown in NB (Nutrient Broth) medium, and *E. coli* HCB136 and HCB137 were grown in LB (Luria-Bertani) medium. Bacterial cells were collected at OD600 values corresponding to the exponential phase (OD600 = 0.8 for ATCC9637, OD600 = 1.2 for HCB136 and HCB137). These sampling points were determined from growth curves based on OD600 and cell concentration measurements (CFU/mL), which confirmed that all three strains were within the exponential growth phase at the time of collection (Fig. 1). The cells were then harvested by centrifugation at 2500g for 10 minutes, washed three times in phosphate buffered saline (PBS, consisting of 0.137 M NaCl, 0.0027 M KCl, 0.01 M Na_2HPO_4, and 0.0018 M KH_2PO_4), and re-diluted in motility buffer at varying cell concentrations. The motility buffer contains 0.01 M potassium phosphate buffer (pH 7) supplemented with 0.067 M NaCl, 10^{-4} M EDTA (ethylenediaminetetraacetic acid), and 0.2 wt% glucose. Prepared sample suspensions were stored in a rotating incubator at 37°C until testing to maintain active *E. coli* motility for the tests.

View Article Online
DOI: 10.1039/D6SM00408C

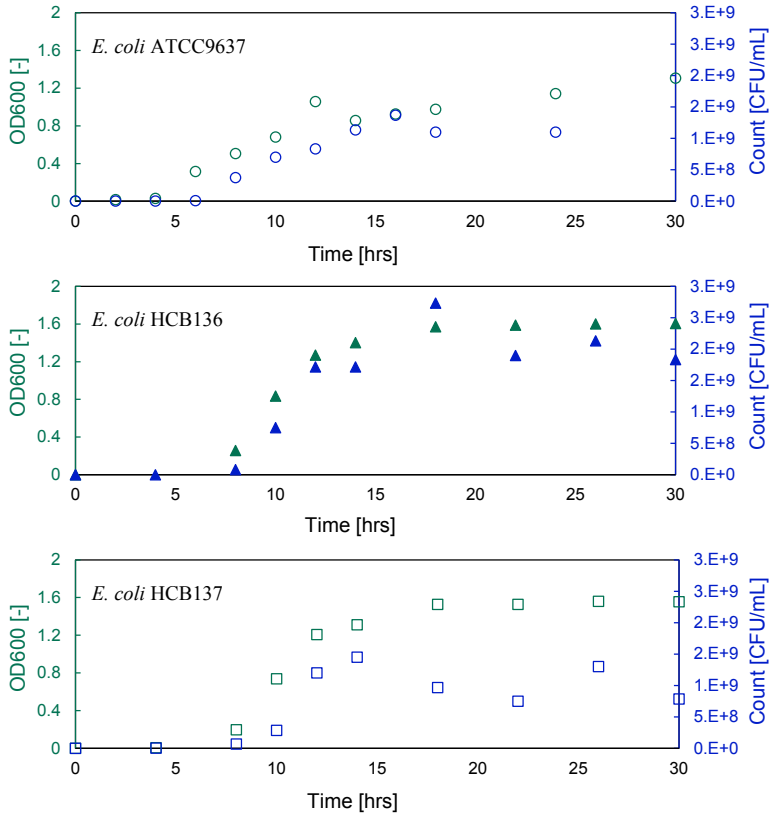

Figure 1. Growth curves based on OD600 and cell concentration for the three tested *E. coli* strains. (a). ATCC9637 (rotating flagella). (b) HCB136 (paralyzed flagella). (c) HCB137 (no flagella).

2.2 Characterization of *Escherichia coli* strains

Morphological analysis was conducted to identify the shape and dimensions of cell bodies and flagella for the *E. coli* strains (Fig. 2). Scanning electron microscopy (SEM) was employed to obtain high-resolution images, and the sample specimens for SEM observation were prepared using the following steps [30]. Bacterial cells were fixed by adding 2.5% glutaraldehyde to the cultivating medium at the exponential phase and then attached to the Poly-l-lysine-coated coverslips. The cells were dehydrated through a graded ethanol series, dried using a critical point dryer (K850, Quorum, UK) with liquid CO_2, and coated with a thin gold layer using a metal sputter (Hummer 6, Anatech, USA).

View Article Online
DOI: 10.1039/D6SM00408C

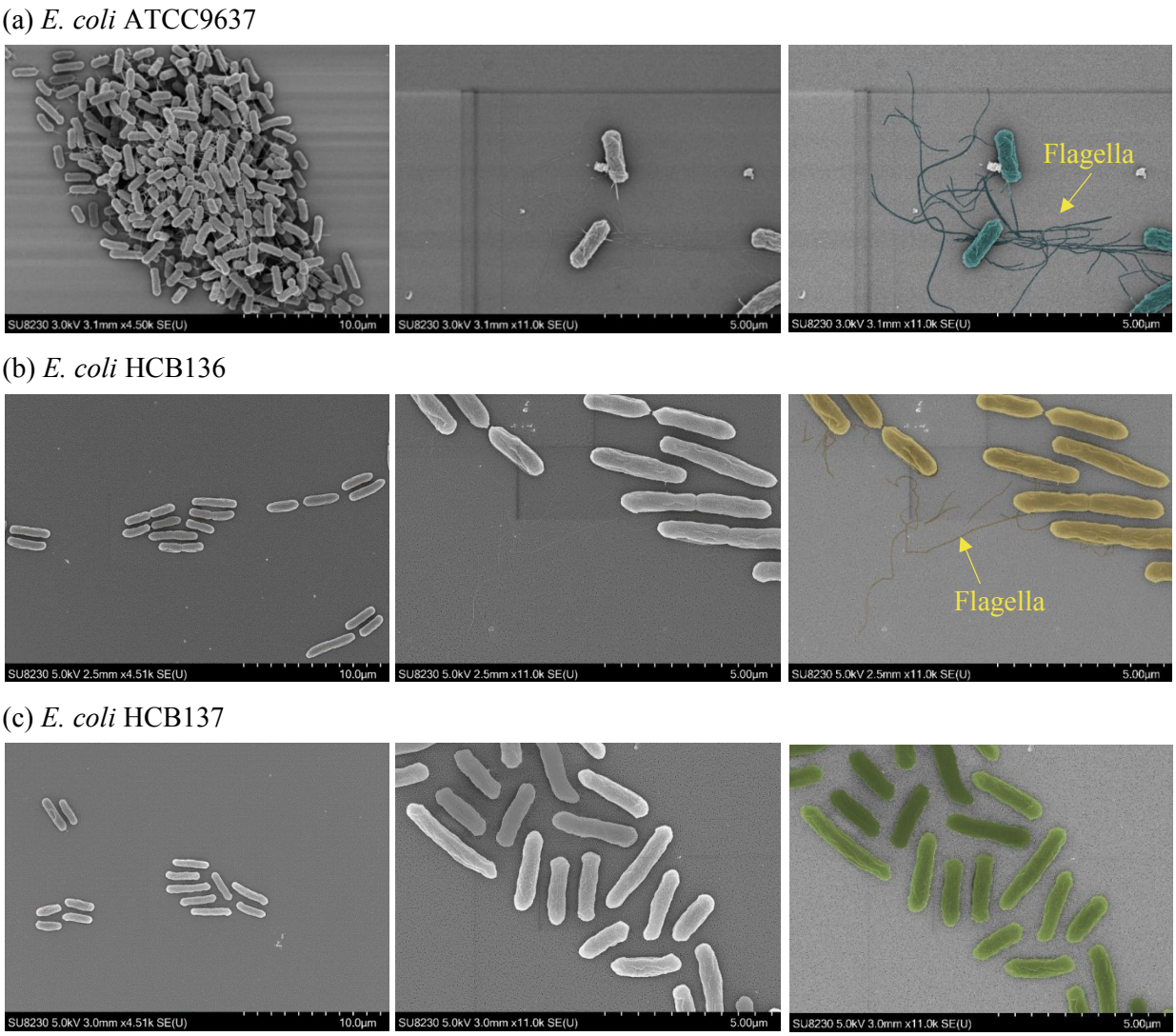

Figure 2. SEM images showing the morphology of three tested *E. coli* strains. (a). ATCC9637 (rotating flagella). (b) HCB136 (paralyzed flagella). (c) HCB137 (no flagella).

We analyzed the trajectories of bacterial swimming to determine the swimming speed of *E. coli* strains (Fig. 3). The movement of cells suspended in motility buffer was captured for 20 seconds using an inverted digital microscope (Zeiss Axio Observer 7, Carl Zeiss AG). The bacterial position was tracked over time, based on which the swimming speed of each strain was subsequently calculated using their cumulative travel distance divided by 20 seconds. It can be seen that ATCC9637 *E. coli* with rotating flagella has a tendency to swim along a certain direction with no obvious pivoting, while HCB136

View Article Online
DOI: 10.1039/D6SM00408C

129 (paralyzed flagella) and HCB137 (no flagella) tend to spin around within a localized region.

130

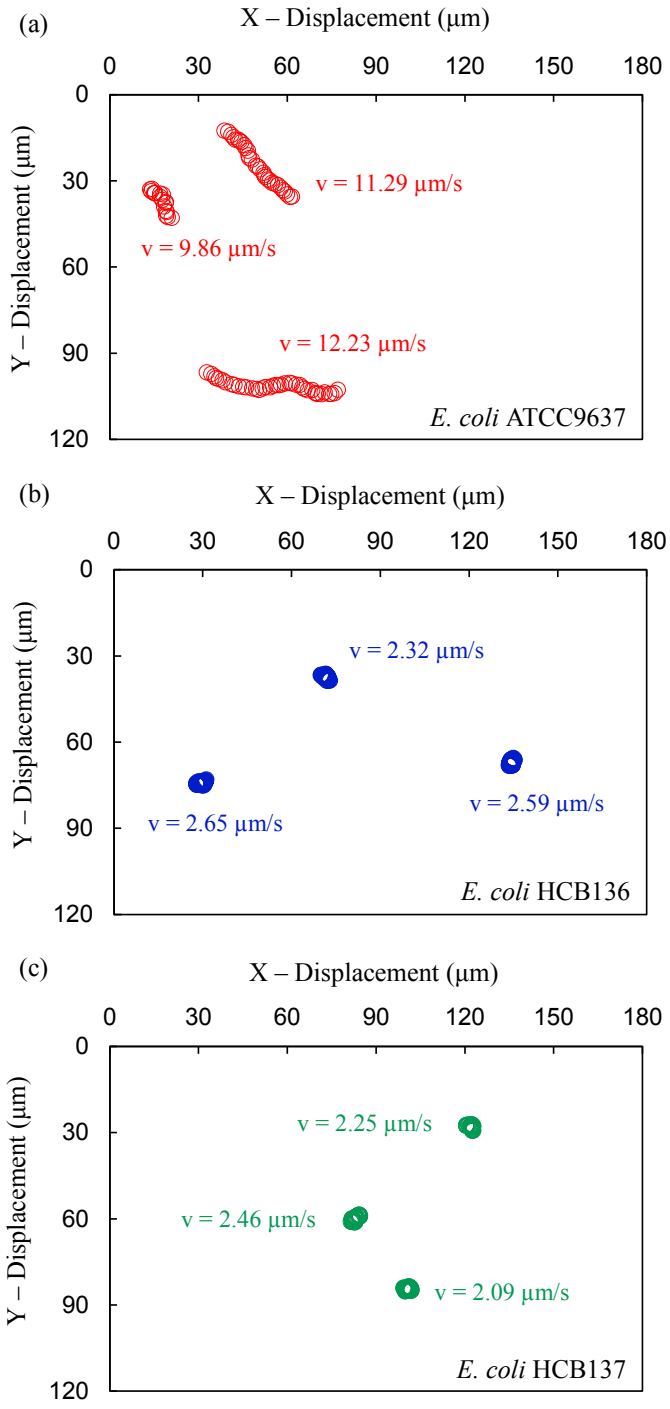

131

132 Figure 3. Estimation of the swimming speed of the three tested *E. coli* strains. (a). ATCC9637 (rotating

133 flagella). (b) HCB136 (paralyzed flagella). (c) HCB137 (no flagella). Open markers show the positions of

View Article Online
DOI: 10.1039/D6SM00408C

tracked *E. coli* in 20 seconds. The velocity v is calculated using the cumulative traveled length divided by 20 seconds of travel time.

2.3 Viscosity measurement

The viscosity of bacterial suspensions at various shear rates was measured using a double-gap Couette geometry (Fig. 4a, MCR302, Anton Paar), which is specifically designed for low-viscous fluids [31]. All viscosity measurements were conducted at 37°C because this is optimal for *E. coli* growth and activity and helps maintain active bacterial motility during testing. The prepared sample suspensions were filled into the gap between the bob and the cup, which was maintained at a temperature of 37°C. Any excess solution was removed to mitigate the impacts of surface tension and capillary action.

The upper bob rotated with a controlled shear rate $\dot{\gamma}$ continuously ranging from 0.01–1000 s^{-1}, while the torque was measured (Fig. 4b). The measurements were conducted under controlled shear rates using a logarithmic ramp-down (i.e., from 1000 to 0.01 s^{-1}) protocol, with 21 logarithmically spaced measurement points, followed by five additional measurements at the lowest shear rate of 0.01 s^{-1}. At each shear rate, the torque was measured after the steady-state criterion of the rheometer was satisfied. The first 21 measurement points required approximately 30 min in total, and the additional five measurements at 0.01 s^{-1} required approximately 5 min. The measured torque was converted into shear stress τ, and then used to calculate the viscosity $\eta = \tau/\dot{\gamma}$. All measurements were repeated in triplicate.

View Article Online
DOI: 10.1039/D6SM00408C

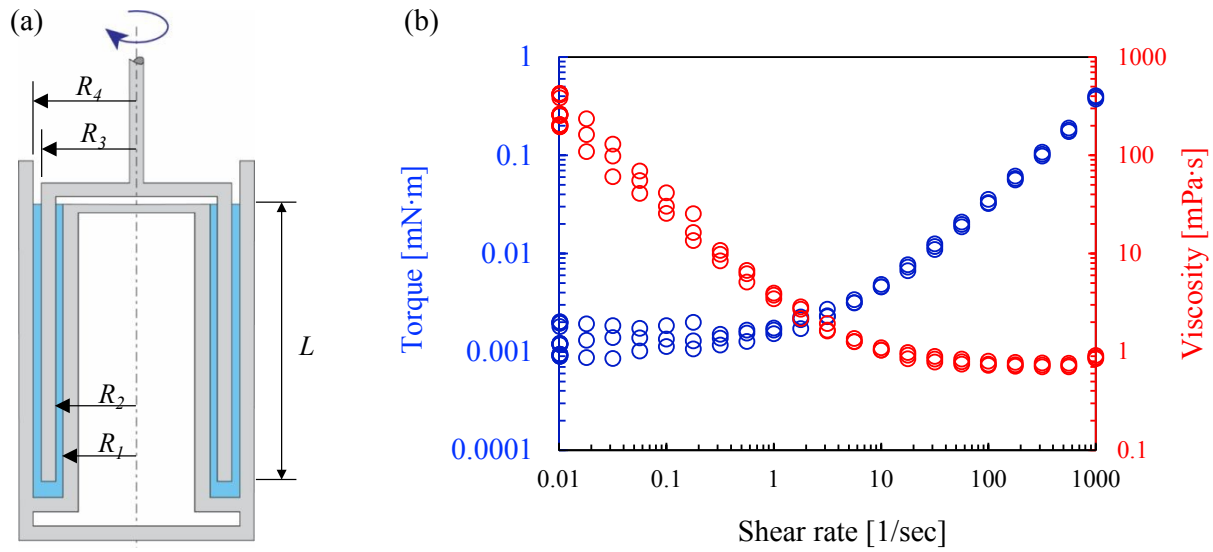

Figure 4. Experimental setup and typical data. (a) The fluid viscosity is measured within a double gap geometry, i.e., Couette flow. R_1 = 19.750mm, R_2 = 20.250mm, R_3 = 21.000mm, R_4 = 21.500mm, and L = 78.700mm. (b) Measured torque at different shear rates for motility buffer without *E. coli* cells at 37°C.

2.4 Model prediction

We employed the Genetic Programming method to discover an equation that can accurately describe and predict the bacterial suspension viscosity. The regression formulation was implemented through a Python package [32, 33]. Through numerous iterative evolutionary and optimization processes, this method stochastically optimized the structure and coefficients of the equation to match the experimental data from a mathematical expression library. We employed five input parameters – cell length l_a, swimming speed V_0, rotational diffusivity d_r, cell volume fraction φ, and shear rate $\dot{\gamma}$ – with the corresponding relative viscosity serving as output data.

3. RESULTS AND DISCUSSION

3.1 Shear rate dependent relative viscosity of three *E. coli* suspensions

The relative viscosity, i.e., suspension viscosity normalized by the viscosity of bacteria-free fluid,

View Article Online
DOI: 10.1039/D6SM00408C

exhibits notable differences among the three *E. coli* strains of ATCC9637, HCB136, and HCB137 as a function of shear rate and cell concentration (Fig. 5).

E. coli ATCC9637 propels itself by rotating its flagella and enables free swimming. As such, the relative viscosity of an *E. coli* ATCC9637 suspension can highlight the influence that motile bacteria exert on fluid viscosity (Fig. 5a). The suspension exhibited a notable reduction in relative viscosity, particularly in the low shear rate regime ($\dot{\gamma} < \sim 1\ \mathrm{s}^{-1}$), followed by shear-thickening and shear-thinning behaviors with an increase in shear rate. The shear-thickening behaviors are more pronounced as the cell concentration increases. In the high shear rate regime ($\dot{\gamma} > \sim 100\ \mathrm{s}^{-1}$), the relative viscosity converged to approximately 1, and the suspension viscosity approached that of the motility buffer. These results align with previous experimental observations that demonstrated the superfluidic regime of active particle suspensions [17, 21, 26]. While these studies evidenced viscosity reduction in bacterial suspensions supplemented with polyvinylpyrrolidone polymer, we here observed a comparable rheological behavior of motile *E. coli* suspension without polymer additives. Theoretical and computational studies have also reported viscosity reduction and nonlinear rheological behavior in active bacterial suspensions [13, 15, 34-36]. These studies generally describe suspension rheology in idealized low-Reynolds-number suspending fluids and therefore may not provide a complete medium-specific interpretation of the present experiments conducted in motility buffer. Nevertheless, they offer insight into how bacterial orientation dynamics and active stress contributions can affect suspension viscosity. In weak flows, bacterial cells can orient themselves and align along the local velocity gradient. Pushers, such as *E. coli*, generate a negative swimming stresslet, which reduces shear stress and consequently decreases the viscosity [13]. As the flow strength increases, bacterial cells tend to align more towards the flow direction. The contribution of active swimming stresses then decreases relative to the Brownian stress (i.e., the stress arises from the random thermal "Brownian" motion of suspended particles and background flow) resulting in shear-thickening and an increase in relative viscosity above 1. Previous studies suggest that at high shear rates, the imposed shear flow becomes sufficiently strong that the stress contributions associated with bacterial activity decay [34, 35]. Consistent with this behavior, the relative viscosity in our experiments decreased after the shear-thickening regime and

View Article Online
DOI: 10.1039/D6SM00408C

197 approached approximately 1, indicating that the bacterial contribution to viscosity became negligible.

198

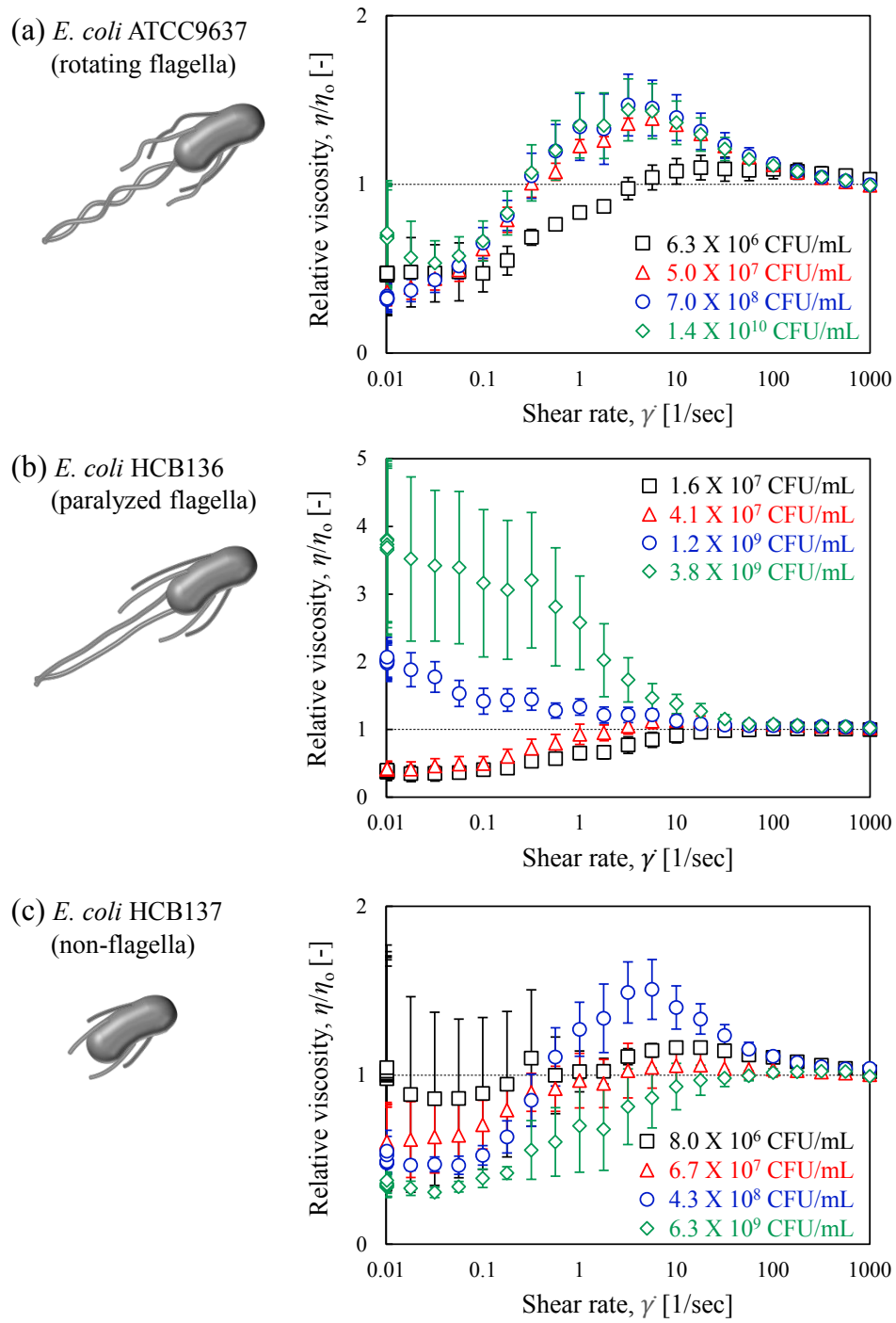

199

200 Figure 5. Relative viscosity of bacterial suspensions of three different *E. coli* strains as a function of shear

201 rate and cell concentration. (a) *E. coli* ATCC9637 with rotating flagella. (b) *E. coli* HCB136 with paralyzed

View Article Online
DOI: 10.1039/D6SM00408C

flagella. (c) *E. coli* HCB137 without flagella.

For *E. coli* HCB136, while morphologically similar to *E. coli* ATCC9637 (Fig. 2a and 2b), their flagella are paralyzed, preventing rotation or self-propulsion, and thus, they are unable to swim freely in the fluid. Consequently, *E. coli* HCB136 exhibited a low displacement speed of merely 2.52 μm/s (compared to 11.13 μm/s of *E. coli* ATCC9637, Fig. 3). Accordingly, the rheological behavior of *E. coli* HCB136 suspension also starkly differs from the suspension with motile *E. coli*, particularly at high bacterial concentrations (Fig. 5b). At diluted concentrations ($C_o \leq 4 \times 10^7$ CFU/mL), *E. coli* HCB136 suspensions exhibit similar rheological behavior to *E. coli* ATCC9637 suspensions, which is characterized by the reduction in viscosity at low shear rates followed by shear-thickening. This similarity may be attributed to their non-spherical shape. Elongated-shaped particles orient along the extensional axis of shear under weak flow conditions [12, 35, 37], and their Brownian diffusion can stretch the fluid, thereby generating extensile stresses [24]. In dilute conditions, where the distance among bacterial cells is larger than the hydrodynamic radius of the cells, interactions among particles are minimal, and the disturbance fields created by individual particles do not significantly alter the overall configuration of the suspension [34, 38]. However, in concentrated conditions, where cell-cell interactions prevail, the interactions with neighboring particles can induce collective motions and chaotic turbulence, depending on the swimming speed of the bacteria. Bacterial dynamics are heavily influenced by noise from tumbling at lower swimming speeds, which can disrupt collective motions [6]. Specifically, in the case of flagellated bacteria that are unable to swim in the prevailing direction, as is the case with *E. coli* HCB136, the effect of turbulent motions can be intensified [39]. At higher bacterial concentrations ($C_o \geq 10^9$ CFU/mL), the relative viscosity increases with increasing shear rate in the low shear rate regime. This increment in viscosity is larger at higher cell concentrations, reaching up to approximately four times the viscosity of the ambient fluid. In the high shear rate regime, bacteria tend to follow the strong fluid flows and the effects of Brownian diffusion or tumbling become minimal, resulting in the relative viscosity converging towards one.

E. coli HCB137 lacks flagella but retains an elongated shape with a high aspect ratio of around 4.5

View Article Online
DOI: 10.1039/D6SM00408C

(Fig. 2c), which is favorable to the emergence of collective behavior. The elongated cells display particle alignment similar to liquid crystals underflow in concentrated populations [40-43]. This collective structure can induce pronounced polarity and strong local flow, often resulting in collective motion faster than the movement of individual cells [6, 39, 44]. This can, in turn, lead to a reduction in viscosity. When the cell concentration is low ($C_o \approx 8 \times 10^6$ CFU/mL), the presence of bacteria exhibits a marginal influence on the relative viscosity of the suspension. The viscosity demonstrates a slight reduction in the low shear rate regime, followed by shear-thickening, and then shear-thinning, with increasing shear rate. However, the overall relative viscosity remains close to one across all shear rate ranges. The impact of collective motion becomes more pronounced as cell concentration increases, leading to greater viscosity reduction at higher cell concentrations within the low shear rate regime. In the mid shear rate regime ($\sim 1\ s^{-1} < \dot{\gamma} < \sim 100\ s^{-1}$), where fluid flow is strong enough to prevent cells from aligning along the shear gradient, the relative viscosity increases. It exhibits shear-thickening followed by shear-thinning or a gradual increase towards ambient fluid viscosity. The emergence of turbulence in this regime does not linearly correlate with cell concentrations. The relationship between the level of turbulence and cell concentrations remains unquantified in this study, yet the findings presented here illustrate that bacterial suspensions display strain-specific rheological behaviors that depend on their morphology and swimming capabilities. The suspension viscosity for all three tested strains is a function of both shear rate and cell concentration.

3.2 Dimensionless analysis of shear viscosity

The relative viscosity of bacterial suspensions does not exhibit a monotonic relationship with shear rates. This nonmonotonic behavior arises from the competition between stresses originating from bacterial movements and from the imposed flow [13, 45]. In weak flow at low shear rate conditions, stresses induced by bacterial motion are relatively more pronounced than those from the imposed flow; hence, *E. coli* motility can significantly influences the fluid viscosity [46]. However, under strong flow at high shear rate conditions, the fluid flow is strong enough that the additional stress contribution from bacterial motility becomes negligible [26]. Consequently, the suspensions behave similarly to their background fluids. To

View Article Online
DOI: 10.1039/D6SM00408C

capture the relative magnitude of the stresses resulting from the flow and from the bacterial swimming activity, a normalized shear rate $\bar{\gamma} = \dot{\gamma}/(V_o/l_a)$, reflecting the shear rates of fluid flow relative to the swimming speed V_o divided by their cell length l_a, is introduced. In addition, we identify two dimensionless numbers, Pe_{f1} and Pe_{f2}, to characterize the approximate boundaries of bacterial stress dominant regime and flow stress dominant regime. $Pe_{f,1}$ represents the relative dimension of the swimming distance between the turnabout ($V_0\tau_R$) to the hydraulic radius of the bacteria (i.e., the length of bacteria, including cell body and flagella), and $Pe_{f,2}$ characterizes the ratio of the advective transport rate and the diffusion rate, respectively:

$$Pe_{f1} = V_0\tau_R/l_a \qquad (1)$$

$$Pe_{f2} = V_0 l_a/D \qquad (2)$$

The estimated values of Pe_{f1} and Pe_{f2} for each *E. coli* strain are provided in Table 1. In this analysis, l_a represents the bacterial cell length including flagella. Since both ATCC9637 and HCB136 are flagellated *E. coli* strains, we assumed a similar effective length of 20 μm for these two strains. This assumption is consistent with previous measurements of the full length of flagellated *E. coli*. López et al. [17] measured the full length of ATCC9637 as approximately 20.7 μm, and Tavaddod et al. [28] reported that the full length of HCB136 ranged from 13 to 21 μm. In contrast, HCB137 lacks flagella, and therefore l_a value was taken as the cell body length measured from SEM images (Fig. 2), which was 2.39 μm. Although l_a is an important geometric parameter, Pe_{f1} and Pe_{f2} are not determined by the cell length alone, but heavily rely on motility related parameters, as shown in Table 1.

Table 1. Size, swimming characteristics, and dimensionless numbers of $Pe_{f,1}$ and Pe_{f2} for three *E. coli* strains. l_a: cell length including the bacterial flagella. V_0: average swimming velocity of bacteria (Fig. 3). D: diffusion coefficient of bacteria. d_r: rotary diffusivity of bacteria. τ_R: reorientation time of bacteria.

E. coli strains	l_a [μm]	V_0 [μm/s]	D [μm²/s]	d_r [rad²/s]	τ_R [s]	Pe_{f1}	Pe_{f2}
ATCC 9637	20	11.13	13[1)]	3 [2)]	0.630 [5)]	0.35	17.1

View Article Online
DOI: 10.1039/D6SM00408C

HCB136	20	2.52	0.243 [3]	0.032[3]	0.230 [5]	0.029	207
HCB137	2.39	2.27	0.291[4]	0.111[3]	0.339[5]	0.32	18.6

Note: 1) Data obtained from [17]. 2) Data obtained from [47] 2) Data obtained from [28]. 3) Data obtained from [25]. 4) Back calculated from the diffusion coefficient, $D = V_0^2\tau_R/6$.

277

278 Fig. 6 shows the relative viscosity of the three *E. coli* strains against the normalized shear rate $\bar{\gamma}$,
279 along with an approximation of the bacterial stress dominant regime, flow stress dominant regime, and
280 transition zone, as indicated by the two characteristic numbers Pe_{f1} and Pe_{f2}.

281

View Article Online
DOI: 10.1039/D6SM00408C

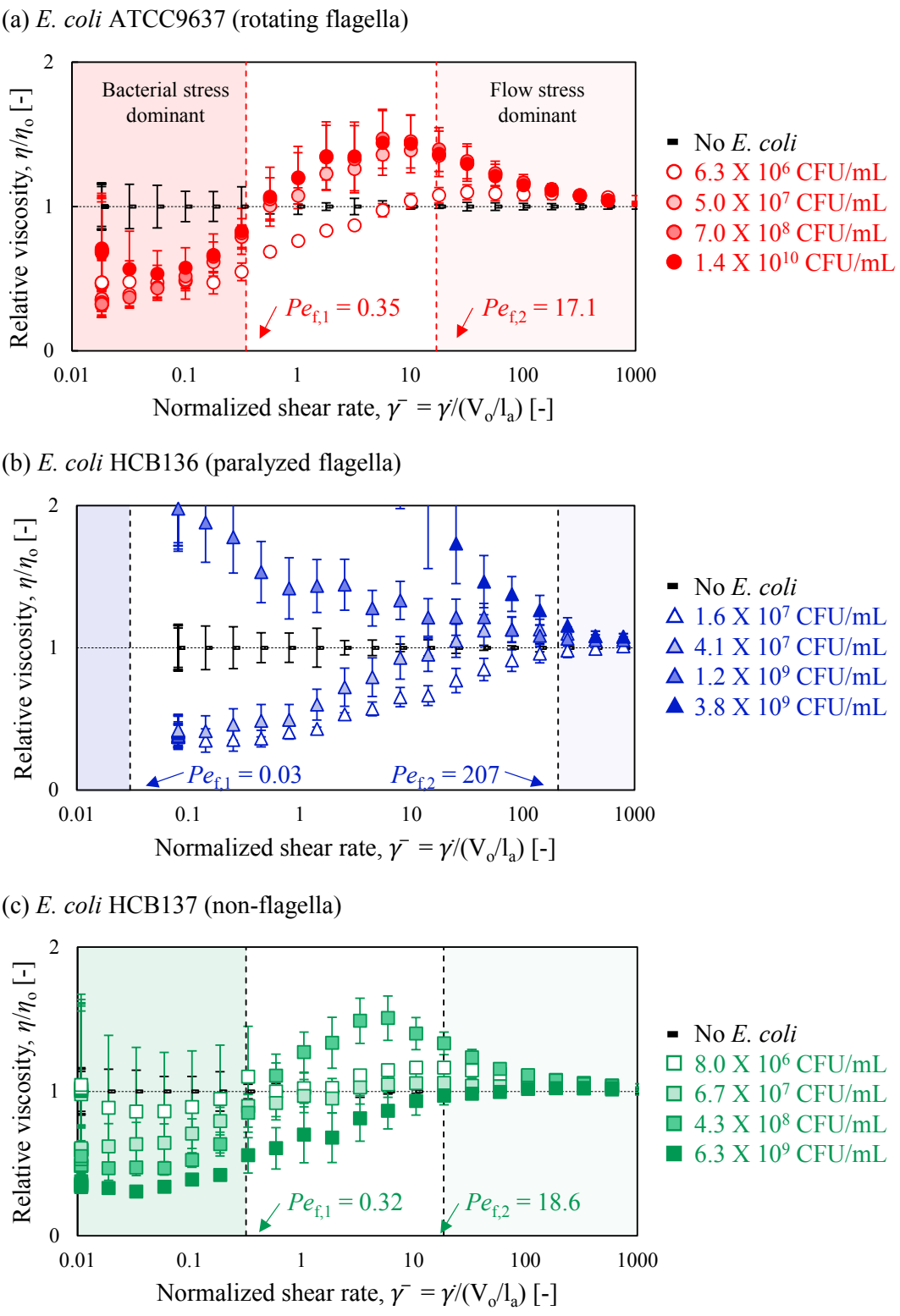

Figure 6. Classification of bacterial stress dominant regime and flow stress dominant regime with Pe_{f1} and Pe_{f2}.

View Article Online
DOI: 10.1039/D6SM00408C

In the characterization of Pe_{f1}, τ_R is defined as the reorientation time of the swimmer, representing the mean duration of the swimmer's free migration time before switching its direction. The reorientation time τ_R can be estimated from its effective swim diffusivity D according to the equation: $\tau_R = 6D/V_o^2$ [35]. The reported values for D are 13 μm²/s for *E. coli* ATCC9637 [17], 0.243 μm²/s for *E. coli* HCB136 [28], and 0.291 μm²/s for *E. coli* HCB137. The resulting reorientation time τ_R is 0.63, 0.23, and 0.34 seconds for each respective strain, leading to Pe_{f1} values of 0.35, 0.029, and 0.32. A larger Pe_{f1} signifies that the bacterial strain can migrate farther from its sphere of influence. The suspensions with *E. coli* ATCC9637 and *E. coli* HCB137, which have Pe_{f1} values more than tenfold greater than *E. coli* HCB136, thus exhibit a wider bacterial stress dominant regime, compared to the *E. coli* HCB136 suspension. When $\bar{\gamma} < Pe_{f1}$, the flow remains relatively weak, allowing the suspension rheology to be influenced by bacteria motility. The micromechanical model to explain the rheology of swimming suspensions [13] anticipates a viscosity reduction at approximately $\dot{\gamma}$ = 0.5 s^{-1}, corresponding to normalized shear rate $\bar{\gamma}$ values of around 0.90, 3.96, and 0.52 for *E. coli* ATCC9637, *E. coli* HCB136, and *E. coli* HCB137 respectively. In addition, the characteristic shear rate $\dot{\gamma}_{c1}$ to identify the viscosity reduction regime in motile *E. coli* suspension is estimated to be around $\dot{\gamma}_{c1}$ = 10 s^{-1} [45], which corresponds to $\bar{\gamma}$ values of approximately 17.97, 79.37, and 10.53 for the three strains, respectively. These numbers are larger than the calculated Pe_{f1} values previously addressed, but they can be suitable for describing diluted *E. coli* suspensions, which feature a wide bacterial stress dominant regime along with a narrow transition zone.

The characterization of Pe_{f2} yields the values of 17.1, 207, and 18.6 for *E. coli* ATCC9637, *E. coli* HCB136, and *E. coli* HCB137, respectively. When $\bar{\gamma}$ exceeds these $Pe_{f,2}$ values, the suspension rheology is dominated by the advective forces from the fluid flow, and particle diffusion plays a relatively minor role. In this regime, the suspension viscosity aligns with the viscosity of the background solution, i.e., the relative viscosity converges to 1. The characteristic shear rate ($\dot{\gamma}_{c2}$) for this Newtonian regime is determined by factors such as the swimming speed, the cell body length, the reorientation time, and the cell volume

View Article Online
DOI: 10.1039/D6SM00408C

fraction [45]. The estimated value is around $\dot{\gamma}_{c2}$ = 50 s^{-1}, which corresponds to normalized shear rate $\bar{\gamma}$ values of approximately 89.85, 396.8, and 52.64 for the three respective strains.

When the normalized shear rate $\bar{\gamma}$ falls between Pe_{f1} and Pe_{f2}, the stress from imposed flow begins to overwhelm the active stress from *E. coli* self-propulsion, and suspension rheology enters a transition zone. Due to the disturbance flow occurring in the opposite direction, the viscosity increases and reaches a maximum [46]. The suspensions of *E. coli* ATCC9637 and *E. coli* HCB137 exhibit their maximum viscosity when the normalized shear rate $\bar{\gamma}$ is around 5, although the specific values vary with bacterial cell concentration.

Paralyzed *E. coli* exhibit completely different motion characteristics compared to swimming *E. coli* or collective particles, and they display unique rheological behavior, as previously presented in Fig. 5. Because of this uniqueness, Pe_{f1} and Pe_{f2} cannot fully describe either the bacterial stress dominant regime or the flow stress dominant regime. The suspension of *E. coli* HCB136 exhibits a Pe_{f1} value about ten times smaller and a Pe_{f2} value about ten times larger than those of the other two *E. coli* suspensions. These unique values result from the comparably small values of swimming speed and diffusion coefficient relative to the hydraulic radius of the cell, a consequence of the presence of paralyzed flagella that contributes little to swimming and instead disturbs the flow.

3.3 Viscosity model for bacterial suspensions

Bacterial suspensions exhibit a non-monotonic viscosity with changing shear rates. Additionally, the viscosity displays variations depending on bacterial strains of different morphology and motility characteristics, as well as cell concentrations. Using Genetic Programming, the bacteria-specific regression model for the relative viscosity η/η_o was derived as:

$$\frac{\eta}{\eta_0} = \left(\frac{d_r}{100} + C_0\right)^{\frac{1.03^{(V_0+d_r)}-(l_a-2.38)C_0}{100\sqrt[3]{d_r}}} \quad (3)$$

where C_o is the cell volume fraction. Admittedly, this model is empirical and incorporates intricate exponents, making it more sophisticated than previously proposed empirical models [12, 21, 24, 45]. This

View Article Online
DOI: 10.1039/D6SM00408C

model should be interpreted as an empirical, data-driven predictive relationship rather than a physically derived model. The equation structure is determined through Genetic Programming process, which generates random mathematical expressions through stochastic equation generation, iterative optimization, and evolutionary refinement. Therefore, final equation structure does not necessarily provide direct physical meaning. Nevertheless, the variables included in the model are physically relevant to bacterial morphology and motility characteristics.

Despite its empirical nature, the model captures the decrease in relative viscosity observed in ATCC9637 and HCB137 suspensions and the increase in relative viscosity in HCB136 suspension. This differs from earlier empirical models that primarily focused on viscosity reduction in motile bacterial suspensions. Fig. 7 presents a comparison of the predicted relative viscosity using Eq. (3) with the measured relative viscosity in the bacterial stress-dominant or low shear rate regime. Given that the viscosity exhibits greater variation in the low shear rate regime and approaches the background viscosity in the high shear rate regime, our analysis primarily emphasizes the comparison in the low shear rate context. As evident in Fig. 7, the predicted values closely align with the 1:1 line, indicating that our developed model reproduce the experimental observations reasonably well.

The predictive model developed here is designed specifically to predict the viscosity of bacterial suspensions with varying morphologies and motility characteristics for both motile and non-motile bacteria, while earlier prediction models primarily focused on motile bacterial suspensions. Although empirical, the Genetic Programming approach successfully captures the diverse rheological behaviors observed in different bacterial suspensions under low shear conditions. The accuracy and robustness of the model may be further improved with an expanded dataset or through additional optimization cycles.

View Article Online
DOI: 10.1039/D6SM00408C

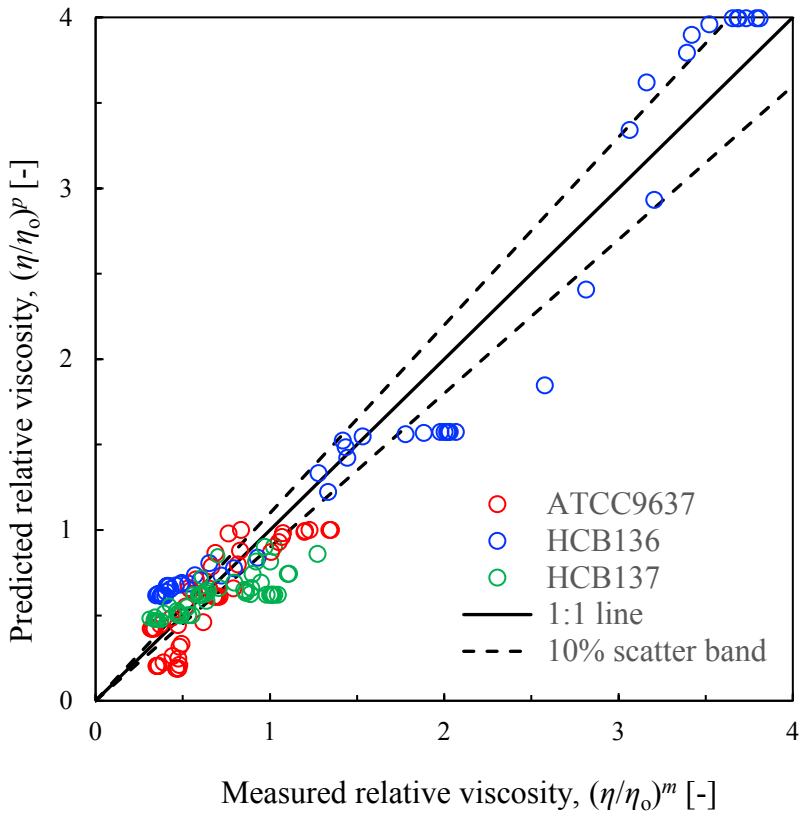

Figure 7. Comparison of measured and predicted relative viscosities in *E. coli* suspensions.

The Genetic Programming approach offers several advantages for the present problem. Because it does not assume a fixed functional form, it can describe rheological responses that vary in sign and shape across strains, capturing both the viscosity reduction of the motile and deflagellated suspensions and the viscosity increase of the paralyzed-flagella suspension within a single expression, which earlier mechanistic empirical models, formulated primarily for viscosity reduction in motile suspensions, do not. The model also relates the relative viscosity to a compact set of physically meaningful inputs spanning morphology and motility, and, as a closed-form symbolic expression, it remains inspectable and differentiable, unlike black-box models.

At the same time, several limitations should be acknowledged. The structure of Eq. (3) is the product of stochastic evolutionary search rather than physical derivation, so its individual terms and fractional exponents do not carry direct mechanistic meaning, and a different random initialization or

View Article Online
DOI: 10.1039/D6SM00408C

operator set could yield an alternative expression of comparable accuracy. As a data-driven relationship fitted to three strains over a finite range of concentrations and emphasizing the low shear rate regime, the model provides prediction rather than mechanistic insight, and extrapolation beyond the tested strains, concentrations, and shear rates is not guaranteed. These constraints suggest that the model is best regarded as a practical predictive tool whose reliability would benefit from a larger and more diverse dataset and from explicit reporting of its domain of validity.

4. CONCLUSIONS

This paper experimentally investigates the suspension viscosity of three *E. coli* strains with distinct morphology and motility characteristics. By comparing a motile strain, a paralyzed-flagella mutant, and a deflagellated mutant in a water-like medium without polymer additives, this work isolates the separate roles of self-propulsion, flagella, and cell shape in suspension rheology, which previous single-strain or motile-only studies failed to distinguish.

The suspension of ATCC 9637, a motile *E. coli* strain, exhibits a notable decrease in viscosity, particularly pronounced in the low shear rate regime. In contrast, the suspension of HCB 136, *E. coli* with paralyzed flagella, shows an increase in viscosity, especially in concentrated suspensions. This contrast underscores the influence of active swimmers in modifying the flow field and subsequently fluid viscosity. The suspension of HCB 137, deflagellated *E. coli*, also displays a reduction in viscosity, despite the absence of the organelles necessary for propulsion. The elongated shape of the cells without flagella facilitates collective behavior, generating substantial local flow, thereby contributing to the decrease in fluid viscosity.

Two dimensionless numbers Pe_{f1} and Pe_{f2} are introduced to delineate the bacterial stress dominant and flow stress dominant regimes along the normalized shear rate. Each *E. coli* suspension manifests unique Pe_{f1} and Pe_{f2} values influenced by various factors, including bacterial cell length, swimming velocity, reorientation time, and diffusion coefficient. Pe_{f1} and Pe_{f2} help elucidate the viscosity behaviors within these regimes for ATCC9637 and HCB137 suspensions, yet they are less

View Article Online
DOI: 10.1039/D6SM00408C

effective in capturing the unique rheology of the HCB136 with paralyzed flagella suspension.

In addition, the genetic programming approach is adopted to devise an empirical model characterizing the viscosity of bacterial suspensions. This viscosity model, as a function of shear rate, cell concentrations, bacterial morphology, and motility characteristics, can successfully approximate the complex rheological behaviors exhibited by the three distinct *E. coli* suspensions studied.

Together, these findings show that bacteria shape and motility, not swimming alone, govern suspension rheology, and that viscosity reduction can occur even without active propulsion. Because the measurements were made in a water-like medium and the model spans both motile and non-motile strains, the results broaden the applicability of active-suspension rheology to the more natural and engineered conditions encountered in environmental, biomedical, and energy-related settings.

View Article Online
DOI: 10.1039/D6SM00408C

ACKNOWLEDGEMENT

The authors thank Prof. Howard C. Berg and Dr. Karen Fahrner at Harvard University for providing the HCB136 and HCB137 *E. coli* strains. This material is based upon work supported by the National Science Foundation (CMMI-1943722). Any opinions, findings and conclusions, or recommendations expressed in this material are those of the authors and do not necessarily reflect those of the NSF. This work was performed in part at the Georgia Tech Institute for Electronics and Nanotechnology, a member of the National Nanotechnology Coordinated Infrastructure (NNCI), which is supported by the National Science Foundation (Grant ECCS-2025462).

View Article Online
DOI: 10.1039/D6SM00408C

REFERENCES

1. Elgeti, J., R.G. Winkler, and G. Gompper, *Physics of microswimmers—single particle motion and collective behavior: a review.* Reports on progress in physics, 2015. **78**(5): p. 056601.
2. Lauga, E. and T.R. Powers, *The hydrodynamics of swimming microorganisms.* Reports on progress in physics, 2009. **72**(9): p. 096601.
3. Alexander, G.P., C. Pooley, and J.M. Yeomans, *Scattering of low-Reynolds-number swimmers.* Physical Review E—Statistical, Nonlinear, and Soft Matter Physics, 2008. **78**(4): p. 045302.
4. Götze, I.O. and G. Gompper, *Mesoscale simulations of hydrodynamic squirmer interactions.* Physical Review E—Statistical, Nonlinear, and Soft Matter Physics, 2010. **82**(4): p. 041921.
5. Ishikawa, T., M. Simmonds, and T.J. Pedley, *Hydrodynamic interaction of two swimming model micro-organisms.* Journal of Fluid Mechanics, 2006. **568**: p. 119-160.
6. Sokolov, A. and I.S. Aranson, *Physical properties of collective motion in suspensions of bacteria.* Physical review letters, 2012. **109**(24): p. 248109.
7. Anderson, J.C., et al., *Environmentally controlled invasion of cancer cells by engineered bacteria.* Journal of molecular biology, 2006. **355**(4): p. 619-627.
8. Oliveira, N.M., K.R. Foster, and W.M. Durham, *Single-cell twitching chemotaxis in developing biofilms.* Proceedings of the National Academy of Sciences, 2016. **113**(23): p. 6532-6537.
9. Felfoul, O., et al., *Magneto-aerotactic bacteria deliver drug-containing nanoliposomes to tumour hypoxic regions.* Nature nanotechnology, 2016. **11**(11): p. 941-947.
10. Haq, B., *The role of microbial products in green enhanced oil recovery: Acetone and butanone.* Polymers, 2021. **13**(12): p. 1946.
11. Miao, S.-J., et al., *Rheological properties of a new microbial exopolysaccharide produced by Sphingomonas sp. HS and its potential in enhanced oil recovery.* Energy & Fuels, 2022. **36**(4): p. 1792-1798.
12. Hatwalne, Y., et al., *Rheology of active-particle suspensions.* Physical review letters, 2004. **92**(11): p. 118101.
13. Saintillan, D., *The dilute rheology of swimming suspensions: A simple kinetic model.* Experimental Mechanics, 2010. **50**(9): p. 1275-1281.
14. Giomi, L., T.B. Liverpool, and M.C. Marchetti, *Sheared active fluids: Thickening, thinning, and vanishing viscosity.* Physical Review E—Statistical, Nonlinear, and Soft Matter Physics, 2010. **81**(5): p. 051908.
15. Haines, B.M., et al., *Effective viscosity of dilute bacterial suspensions: a two-dimensional model.* Physical biology, 2008. **5**(4): p. 046003.
16. Haines, B.M., et al., *Three-dimensional model for the effective viscosity of bacterial suspensions.* Physical Review E—Statistical, Nonlinear, and Soft Matter Physics, 2009. **80**(4): p. 041922.
17. López, H.M., et al., *Turning bacteria suspensions into superfluids.* Physical review letters, 2015. **115**(2): p. 028301.
18. Sokolov, A. and I.S. Aranson, *Reduction of viscosity in suspension of swimming bacteria.* Physical review letters, 2009. **103**(14): p. 148101.
19. Rafaï, S., L. Jibuti, and P. Peyla, *Effective viscosity of microswimmer suspensions.* Physical Review Letters, 2010. **104**(9): p. 098102.
20. Karmakar, R., et al., *Motor characteristics determine the rheological behavior of a suspension of microswimmers.* Physics of Fluids, 2014. **26**(7).
21. Chui, J.Y., et al., *Rheology of bacterial superfluids in viscous environments.* Soft Matter, 2021. **17**(29): p. 7004-7013.
22. Guo, S., et al., *Symmetric shear banding and swarming vortices in bacterial superfluids.* Proceedings of the National Academy of Sciences, 2018. **115**(28): p. 7212-7217.
23. Hayano, H. and A. Furukawa, *Hydrodynamic interactions in anomalous rheology of active suspensions.* Physical Review Research, 2022. **4**(4): p. 043091.
24. Takatori, S. and J. Brady, *Superfluid behavior of active suspensions from diffusive stretching.*

View Article Online
DOI: 10.1039/D6SM00408C

Physical review letters, 2017. **118**(1): p. 018003.
25. McClaine, J.W. and R.M. Ford, *Characterizing the adhesion of motile and nonmotile Escherichia coli to a glass surface using a parallel-plate flow chamber.* Biotechnology and Bioengineering, 2002. **78**(2): p. 179-189.
26. Gachelin, J., et al., *Non-Newtonian viscosity of Escherichia coli suspensions.* Physical review letters, 2013. **110**(26): p. 268103.
27. Liu, J., R.M. Ford, and J.A. Smith, *Idling time of motile bacteria contributes to retardation and dispersion in sand porous medium.* Environmental science & technology, 2011. **45**(9): p. 3945-3951.
28. Tavaddod, S., et al., *Probing passive diffusion of flagellated and deflagellated Escherichia coli.* The European Physical Journal E, 2011. **34**(2): p. 16.
29. Johnston, M.T. and R.H. Ewoldt, *Precision rheometry: Surface tension effects on low-torque measurements in rotational rheometers.* Journal of Rheology, 2013. **57**(6): p. 1515-1532.
30. Gluenz, E., et al., *Scanning and three-dimensional electron microscopy methods for the study of Trypanosoma brucei and Leishmania mexicana flagella*, in *Methods in cell biology*. 2015, Elsevier. p. 509-542.
31. Marín-Santibáñez, B.n.M., et al., *The Double-Gap Couette Viscometer: An Accurate Tool To Determine the Intrinsic Viscosity and Viscosity-Average Molecular Weight of Polymers.* Industrial & Engineering Chemistry Research, 2025. **64**(39): p. 19210-19221.
32. Im, J., et al., *Data-driven discovery of the governing equations for transport in heterogeneous media by symbolic regression and stochastic optimization.* Physical Review E, 2023. **107**(1): p. L013301.
33. Im, J., et al., *Application of genetic programming for model-free identification of nonlinear multi-physics systems.* Nonlinear Dynamics, 2021. **104**(2): p. 1781-1800.
34. Koch, D.L. and G. Subramanian, *Collective hydrodynamics of swimming microorganisms: living fluids.* Annual Review of Fluid Mechanics, 2011. **43**(1): p. 637-659.
35. Saintillan, D., *Rheology of active fluids.* Annual review of fluid mechanics, 2018. **50**: p. 563-592.
36. Marchetti, M.C., et al., *Hydrodynamics of soft active matter.* Reviews of modern physics, 2013. **85**(3): p. 1143-1189.
37. Jeffery, G.B., *The motion of ellipsoidal particles immersed in a viscous fluid.* Proceedings of the Royal Society of London. Series A, Containing papers of a mathematical and physical character, 1922. **102**(715): p. 161-179.
38. Subramanian, G. and D.L. Koch, *Critical bacterial concentration for the onset of collective swimming.* Journal of Fluid Mechanics, 2009. **632**: p. 359-400.
39. Cisneros, L.H., et al., *Dynamics of swimming bacteria: Transition to directional order at high concentration.* Physical Review E—Statistical, Nonlinear, and Soft Matter Physics, 2011. **83**(6): p. 061907.
40. Peruani, F., A. Deutsch, and M. Bär, *Nonequilibrium clustering of self-propelled rods.* Physical Review E—Statistical, Nonlinear, and Soft Matter Physics, 2006. **74**(3): p. 030904.
41. Großmann, R., I.S. Aranson, and F. Peruani, *A particle-field approach bridges phase separation and collective motion in active matter.* Nature communications, 2020. **11**(1): p. 5365.
42. Bär, M., et al., *Self-propelled rods: Insights and perspectives for active matter.* Annual Review of Condensed Matter Physics, 2020. **11**(1): p. 441-466.
43. Cisneros, L.H., et al., *Fluid dynamics of self-propelled microorganisms, from individuals to concentrated populations.* Experiments in Fluids, 2007. **43**(5): p. 737-753.
44. Méhes, E. and T. Vicsek, *Collective motion of cells: from experiments to models.* Integrative biology, 2014. **6**(9): p. 831-854.
45. Xu, X., et al., *Experimental study on shear viscosity and rheopexy of Escherichia coli suspensions.* Rheologica Acta, 2022. **61**(4): p. 271-280.
46. Alonso-Matilla, R., B. Ezhilan, and D. Saintillan, *Microfluidic rheology of active particle suspensions: Kinetic theory.* Biomicrofluidics, 2016. **10**(4).

View Article Online
DOI: 10.1039/D6SM00408C

516 47. Berg, H. C. 1993. Random walks in biology: Princeton University Press.

View Article Online
DOI: 10.1039/D6SM00408C

Data for this article are available at FigShare:

Dai, Sheng C (2026). Dataset - Rheology of *Escherichia coli* suspensions with various bacterial appearance and motion characteristics. figshare. Dataset.
https://doi.org/10.6084/m9.figshare.32147557